ELSEVIER

1 March 1997

OPTICS COMMUNICATIONS

Optics Communications 136 (1997) 114–124

Full length article

Plane wave spectrum of electromagnetic beams

A. Doicu [1], T. Wriedt

Institut für Werkstofftechnik, Badgasteinerstr. 3, 28259 Bremen, Germany

Received 17 May 1996; revised version received 30 August 1996; accepted 14 October 1996

Abstract

A plane wave spectrum method of Gaussian beams can be derived by using Davis' approximations for the vector potential. An equivalent vector potential is introduced by considering the inverse Fourier transform of the spectrum function of the original vector potential in a given plane. The electromagnetic field, which corresponds to the equivalent vector potential, satisfies Maxwell's equations and can be written as a sum of plane waves. The beam shape coefficients, or the expansion coefficients in terms of regular spherical vector wave functions, are expressed as simple integrals. This version of the plane wave spectrum method offers the possibility to compute higher-order corrections for Gaussian beams.

1. Introduction

The scattering problem of Gaussian beams by arbitrarily shaped particles is of importance in various fields of optics. In order to obtain the exact solution of the scattering problem the numerical methods for electromagnetic scattering had to be modified to integrate the Gaussian beam description. Our presentation will be focused on the possibilities of implementing Gaussian beam descriptions in the extended boundary condition method [1]. There are two methods available, which rely on the decomposition of the incident field into an infinite series of elementary constituents, such as partial waves [2–6] or plane waves [7–11], with amplitudes and phases given by a set of beam shape coefficients. Some limitations of these methods for Gaussian beam scattering by arbitrarily shaped particles will be discussed below.

The partial waves decomposition method consists of the expansion of a Gaussian beam in terms of spherical vector wave functions. This method is based on Davis' description of Gaussian beams [12], accounting for axial and transverse field components. Each nth Davis beam appears under three versions which are the mathematical conservative version, the L-version and the symmetrized version. None of these beams are exact solutions of Maxwell's equations, so that each nth Davis beam can be considered as a "pseudo-electromagnetic" field. It is well known that the expansion in terms of spherical vector wave functions, which are solutions of Maxwell's equations, is problematic when the electromagnetic description of the Gaussian beams does not perfectly satisfy Maxwell's equations. In the partial waves decomposition method the pseudo-electromagnetic field is replaced by an equivalent electromagnetic field having the same values as the original field on a given spherical surface. As a consequence of the equivalence method the beam shape coefficients, expressed as surface integrals, depend on the radius of the spherical surface where the boundary conditions were imposed. This influence is significant for tightly focused Gaussian beams. For spherical particles the equivalence surface is identical to the particle surface. The completeness and the orthogonality of the spherical harmonics functions on spherical surfaces make this choice to be valid. But for arbitrarily shaped particles the choice of the equivalence surface is problematic. We note here, that for a weakly focused Gaussian beam the generalized localized approximation to the beam shape coefficients

[1] E-mail: doicu@iwt.uni-bremen.de.

PII S0030-4018(96)00641-4

represents a pleasing alternative [4]. This is not a rigorous method but it represents a great simplification in Gaussian beam scattering and reduces many times the computing time required for its implementation.

The plane wave spectrum method can be used to model any physically realizable beam, whether or not the beam has an analytical representation. The classical method, which uses the angular spectrum of plane waves to model an arbitrary beam, is based on Kogelnick and Li's description of the fundamental mode of a Gaussian beam [13]. In this representation of laser beams only the transverse component of the electric field is taken into account. The "pseudo-electromagnetic" field is replaced by an equivalent electromagnetic field by considering the inverse Fourier transform of the spectrum function of the original field in a given plane [14]. The equivalence is performed in such a way that one assures the equality between the values of the fields in a given plane. Although the longitudinal field component is not included in the field expressions, the first-order correction to it is taken into account when the plane wave spectrum representation of the beam is derived. In practice, the axial component of the equivalent electromagnetic field is obtained by imposing an additional condition, namely the divergence condition. The major limitation of the plane wave spectrum method consists in a lack of a procedure for obtaining higher-order corrections of the Gaussian beam. This limitation restricts the applicability of the method to weakly focused Gaussian beams. It is well known that the accuracy of the Gaussian beam description depends on the beam parameter s [12], since the exponent of s characterizes the order of approximation. According to Ref. [15], the first order is accurate to $s < 0.07$, while the fifth-order is accurate to $s < 0.2$, if the maximum percent error of the solution to Maxwell's equations should not exceed 1.2%. It is obvious that the only conditions for detectable differences among various models are in focused scattering, i.e. forward diffraction, rainbows and glory scattering.

The main contribution of the present paper is our new version of the plane wave spectrum method whereby we are able to compute higher-order corrections of Gaussian beams. By considering the Davis approximation for the vector potential and by using the Fourier transform we construct an equivalent vector potential which satisfies the wave equation. The relative simplicity of our method originates from the fact that we deal with the vector potential $\boldsymbol{A}$. Contrarily, the classical version of the plane wave spectrum method uses the electric field and necessitates to consider the equivalence for $\boldsymbol{E}$. This procedure leads to ambiguities because, for a given order of approximation, there are several possibilities to choose the field components which will be Fourier transformed. The electromagnetic field which corresponds to the equivalent vector potential is divergence free and can be written as a superposition of plane waves. The benefit of the present procedure consists also in the fact that the equivalent electromagnetic field can be exactly expanded in terms of spherical vector wave functions.

2. Development of the formalism

In the Davis procedure one assumes the vector potential of the beam to be linearly polarized in the x-direction [12]

$$\boldsymbol{A}(\boldsymbol{r}, t) = A(\boldsymbol{r}) \exp(\mathrm{i}\omega t)\, \boldsymbol{e}_x, \tag{1}$$

so that the non-vanishing component of $\boldsymbol{A}$ obeys a scalar wave equation

$$\nabla^2 A(\boldsymbol{r}) + k^2 A(\boldsymbol{r}) = 0. \tag{2}$$

For a focused Gaussian beam $A(\boldsymbol{r})$ is taken to be of the form

$$A(\boldsymbol{r}) = \frac{\mathrm{i}E_0}{k}\psi(\boldsymbol{r}) \exp(\mathrm{i}kz), \tag{3}$$

where the slowly varying function $\psi(\boldsymbol{r})$ satisfies the following differential equation

$$\nabla^2\psi + 2\mathrm{i}k\partial\psi/\partial z = 0. \tag{4}$$

The solution of this equation may be written as a series in powers of s^2 as

$$\psi(\boldsymbol{r}) = \psi_0(\boldsymbol{r}) + s^2\psi_2(\boldsymbol{r}) + \ldots, \tag{5}$$

where s is the beam parameter equal to the waist radius w_0 divided by the diffraction length l, $s = w_0/l = 1/(kw_0)$. In terms of rectangular coordinates normalized to w_0 and l

$$\xi = \frac{x}{w_0}, \quad \eta = \frac{y}{w_0}, \quad \zeta = \frac{z}{l} = s\,\frac{z}{w_0}, \tag{6}$$

the lowest-order functions ψ_0 and ψ_2 are given by

$$\psi_0 = \mathrm{i}Q \exp(-\mathrm{i}Q\rho^2), \quad \psi_2 = (2\mathrm{i}Q + \mathrm{i}\rho^4 Q^3)\psi_0, \quad \rho^2 = \xi^2 + \eta^2, \quad Q = 1/(\mathrm{i} - 2\zeta). \tag{7}$$

If the center of the focal waist is located at the point (x_0, y_0, z_0), $A(x, y, z)$ can be written as

$$A(x, y, z) = \frac{iE_0}{k}\psi(x-x_0, y-y_0, z-z_0)\exp[ik(z-z_0)]. \tag{8}$$

The non-vanishing component of the vector potential, which was obtained by considering only the lowest-order functions ψ_0 and ψ_2, is not an exact solution of the scalar wave equation. This vector potential will be replaced by an equivalent vector potential which satisfies the wave equation [14].

Eq. (8) can be Fourier transformed at an arbitrarily given plane $z = z_1$ to yield the spectrum function of $A(x, y, z)$, i.e.

$$\begin{aligned}\tilde{A}(k_x, k_y) &= \int_{-\infty}^{\infty}\int_{-\infty}^{\infty} A(x, y, z)\exp[-i(xk_x + yk_y)]\,dx\,dy \\ &= \left(\frac{iE_0}{k}\right)\pi w_0^2\exp[ik(z-z_0)]\left[1 + s^2 w_0^2\left(\left(k_x^2+k_y^2\right) - \frac{w_0^2}{16\,i\bar{Q}}\left(k_x^2+k_y^2\right)^2\right)\right] \\ &\quad\times\exp[-i(x_0k_x + y_0k_y)]\exp\left(-\frac{w_0^2}{4i\bar{Q}}\left(k_x^2+k_y^2\right)\right),\end{aligned} \tag{9}$$

where $\bar{Q} = 1/[i - 2(z_1 - z_0)/l]$.

The non-vanishing component of the equivalent vector potential, written as

$$A_0(x, y, z) = \frac{1}{4\pi^2}\int_{-\infty}^{\infty}\int_{-\infty}^{\infty}\tilde{A}(k_x, k_y)\exp\{i[xk_x + yk_y + (z-z_1)k_z]\}\,dk_x\,dk_y, \tag{10}$$

where $k_x^2 + k_y^2 + k_z^2 = 1$, satisfies the scalar wave equation and the boundary condition at the $z = z_1$ plane

$$A_0(x, y, z_1) = F^{-1}[\tilde{A}(k_x, k_y)](x, y) = A(x, y, z_1). \tag{11}$$

In the expansion of the vector potential we have considered only the zeroth- and second-order terms. We note that it is a simple problem of algebra to derive the expression of the equivalent vector potential if the fourth-order correction in Eq. (5) is taken into account.

If $|k_x| > k$, then either k_y, k_z or both k_y and k_z must be complex. Similarly, if $|k_y| > k$, then either k_x, k_z or both k_x and k_z must be complex. Consequently, if the limits of integration in Eq. (17) are $\pm\infty$, then a fraction of the plane waves are inhomogeneous. We choose the limits of integration in Eq. (17) so that k_x, k_y and k_z are always real, i.e. all real k_x, k_y such that $k_x^2 + k_y^2 < k^2$ are included. This choice has little or no practical significance except in cases where w_0 is chosen to be significantly smaller than a wavelength. The fact that $|k_x|$ and $|k_y|$ are smaller than k means that the beam is actually a Gaussian function convolved with a spread function [8]. In Fig. 1 we have compared the values of the Davis vector potential with the values of the equivalent vector potential computed by using the integral representation (10) in which we have restricted the integration domain to $k_x^2 + k_y^2 < k^2$. For simplicity, we considered an on-axis beam. The comparison was performed in the $z = 0$ plane for different orders of approximation and various values of the beam parameter s. For larger values of s, the equivalent vector potential deviates from a Gaussian profile, but for $s < 0.1$ the limitation of the integration domaine to real k_x and k_y has no significant effect. Indeed, for the Davis second-order approximation, the magnitude of the average deviation of the ratio A_0/A from unity, extending over $0 < \rho < 2.65$, is about 1.222×10^{-6} for $s = 0.11$, and about 2.937×10^{-7} for $s = 0.032$.

The electric field of the beam can be expressed in terms of A_0 as follows

$$E(x, y, z) = (-ik)\left[\left(A_0 + \frac{1}{k^2}\frac{\partial^2 A_0}{\partial x^2}\right)e_x + \frac{1}{k^2}\frac{\partial^2 A_0}{\partial x\partial y}e_y + \frac{1}{k^2}\frac{\partial^2 A_0}{\partial x\partial z}e_z\right], \tag{12}$$

or, due to the fact that the exponential term $\exp[-w_0^2(k_x^2 + k_y^2)/(4i\bar{Q})]$ vanishes faster than other polynomial function in Eq. (9), the order of differentiation and integration can be interchanged to obtain

$$E(x, y, z) = (-ik)\frac{1}{4\pi^2}\iint_{k_x^2+k_y^2\le k^2} V_0(k_x, k_y, k_z)\,\tilde{A}(k_x, k_y)\exp(ikr)\exp(-ik_z z_1)\,dk_x\,dk_y, \tag{13}$$

where

$$V_0(k_x, k_y, k_z) = \left(1 - \frac{k_x^2}{k^2}\right)e_x - \frac{k_xk_y}{k^2}e_y - \frac{k_xk_z}{k^2}e_z. \tag{14}$$

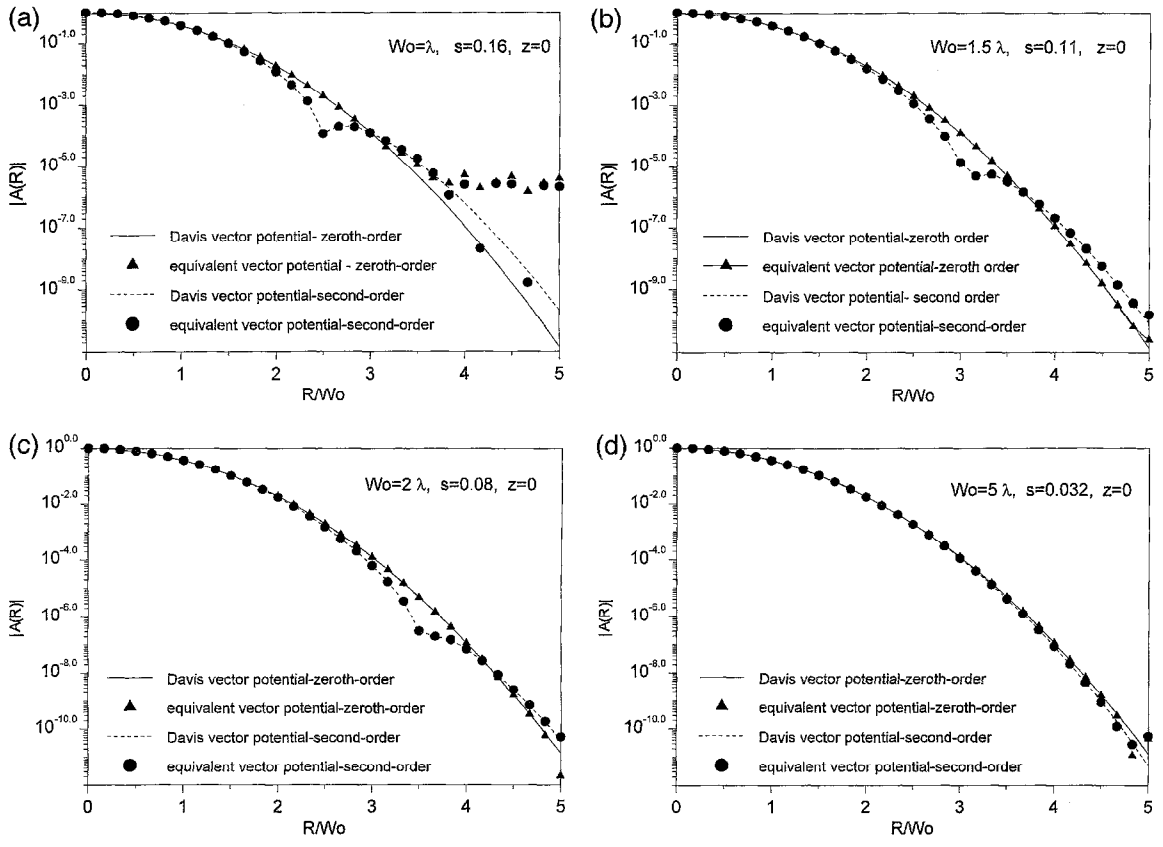

Fig. 1. Davis vector potential and equivalent vector potential in the $z = 0$ plane for different orders of approximation and various values of the beam parameter s.

The integrand in Eq. (13) can be viewed as a plane wave with the amplitude $V_0(k_x, k_y, k_z)\,\tilde{A}(k_x, k_y)\exp(-ik_z z_1)$ and the propagation vector $\boldsymbol{k}(k_x, k_y, k_z)$. The expression of Eq. (13) is our version of the plane wave spectrum representation of Gaussian beams. It can be simply demonstrated that the divergence condition of the electric field is satisfied and that $\boldsymbol{V}_0 \cdot \boldsymbol{k} = 0$.

The classical plane wave spectrum representation can be obtained by replacing $\boldsymbol{V}_0$, given in Eq. (14), by $\boldsymbol{V}_0 = \boldsymbol{e}_x - (k_x/k_z)\boldsymbol{e}_z$ and by neglecting the terms with powers of s equal to 2 in the expression of $\tilde{A}(k_x, k_y)$. This procedure corresponds to the zeroth-order Davis approximation of the vector potential. In order to show the significance of the higher-order corrections for tightly focused Gaussian beams, we have computed the relative error percentage by taking the percental deviations of the magnitude of the left-hand side of Eq. (2) from zero relative to A. Table 1 provides a comparison of the maximum error percentage for $s = 0.032$; 0.053; 0.08 and $s = 0.11$ for zeroth- and second-order Davis approximations of the vector potential. The maximum error percentage was calculated in the $z = 0$ plane for $0 < \rho < 1.5$. As shown in Table 1, the second-order approximation yields a significant improvement in accuracy in comparison to the commonly used

Table 1
Maximum error percentage of solution to Eq. (4) for zeroth- and second-order Davis approximation of the vector potential. Error percentage calculated in the $z = 0$ plane for $0 < \rho < 1.5$

Beam parameter s	Maximum error zeroth-order [%]	Maximum error second-order [%]
0.032	0.819	0.008
0.053	2.247	0.064
0.08	5.12	0.335
0.11	9.68	1.2

zeroth-order description. According to these calculations, the Davis second-order approximation can be used for s less than about 0.1, if a deviation of 1% is acceptable.

The scattering problem can be solved for each of these plane wave components by using the extended boundary condition method and the technique described in Refs. [9–11], i.e. the total scattering field pattern due to the incident Gaussian beam will be found by summing over a continuous superposition of such solutions.

3. Integral representations for the beam shape coefficients

In order to obtain convergent results, a significant number of plane waves must be considered in the angular spectrum of the Gaussian beam. In this case the computing time is substantial. A simplification in Gaussian beam scattering, in the view of the extended boundary condition method, represents the expansion of the incident wave in terms of spherical vector wave functions. In this case the coefficients of the scattered field are related to the beam shape coefficients by the transition matrix [1].

Instead of directly expanding the "pseudo-electromagnetic" field as a series of spherical vector wave functions, we will use the equivalent electromagnetic field derived in the plane wave spectrum representation of Gaussian beams. The field defined in Eq. (13) is an electromagnetic field corresponding to a given order of approximation for the vector potential. Due to the fact that this field is an exact solution of Maxwell's equations, an expansion in terms of spherical vector wave functions can be exactly performed.

To evaluate the integral we use the spherical coordinate angles α and β: $k_x = k \sin\alpha \cos\beta$, $k_y = k \sin\alpha \sin\beta$, $k_z = k \cos\alpha$, so that Eq. (13) can be rewritten in the form

$$\boldsymbol{E}(x, y, z) = (-\mathrm{i}k)\frac{1}{4\pi^2}\int_0^{\pi/2}\int_0^{2\pi} V_0(\alpha, \beta)\, \tilde{\boldsymbol{A}}(k \sin\alpha \cos\beta, k \sin\alpha \sin\beta) \times \exp(-\mathrm{i}k \cos\alpha\, z_1) \exp(\mathrm{i}\boldsymbol{kr}) k^2 \sin\alpha \cos\alpha \, \mathrm{d}\alpha \, \mathrm{d}\beta. \tag{15}$$

Each plane wave component of the integrand can be represented as a series of spherical vector wave functions of the first kind

$$V_0(\alpha, \beta) \exp(\mathrm{i}\boldsymbol{kr}) = \sum_{n=1}^{\infty}\sum_{m=-n}^{n} D_{mn}\left[a_{mn}\boldsymbol{M}_{mn}^1(\boldsymbol{kr}) + b_{mn}\boldsymbol{N}_{mn}^1(\boldsymbol{kr})\right], \tag{16}$$

where D_{mn} is a normalization constant, and [1]

$$a_{mn} = 4\mathrm{i}^n V_0\left[-\mathrm{i}m\frac{P_n^m(\cos\alpha)}{\sin\alpha}\boldsymbol{e}_\theta - \frac{\mathrm{d}P_n^m(\cos\alpha)}{\mathrm{d}\alpha}\boldsymbol{e}_\varphi\right]\exp(-\mathrm{i}m\beta),$$

$$b_{mn} = -4\mathrm{i}^{n+1} V_0\left[\frac{\mathrm{d}P_n^m(\cos\alpha)}{\mathrm{d}\alpha}\boldsymbol{e}_\theta - \mathrm{i}m\frac{P_n^m(\cos\alpha)}{\sin\alpha}\boldsymbol{e}_\varphi\right]\exp(-\mathrm{i}m\beta), \tag{17}$$

$$\boldsymbol{e}_\theta = \cos\alpha\cos\beta\,\boldsymbol{e}_x + \cos\alpha\sin\beta\,\boldsymbol{e}_y - \sin\alpha\,\boldsymbol{e}_z, \quad \boldsymbol{e}_\varphi = -\sin\beta\,\boldsymbol{e}_x + \cos\beta\,\boldsymbol{e}_y$$

The Legendre functions which appear in Eqs. (16), (17) are defined for negative and positive values of the index m [16].

By substituting Eq. (16) into Eq. (15) and performing the integration over β, we obtain the expansion of the electric field in terms of spherical vector wave functions of the first kind

$$\boldsymbol{E}(\boldsymbol{r}) = E_0 \sum_{n\geq 1}\sum_{m=-n}^{n} C_{nm}\left[\mathrm{i}\, g_{n,\mathrm{TE}}^m\, \boldsymbol{M}_{mn}^1(\boldsymbol{kr}) + g_{n,\mathrm{TM}}^m\, \boldsymbol{N}_{mn}^1(\boldsymbol{kr})\right]. \tag{18}$$

The C_{nm} coefficients are normalization factors for negative values of the index m, which we have introduced to assure the compatibility between our formalism and the classical one [2–5]

$$C_{nm} = \begin{cases} C_n, & m \geq 0 \\ (-1)^{|m|}\dfrac{(n+|m|)!}{(n-|m|)!}\, C_n, & m < 0 \end{cases} \tag{19}$$

The coefficients C_n are found in the Bromwich formulation of the Lorenz-Mie theory and are defined in Refs. [1–4]

$$C_n = \mathrm{i}^{n-1}\frac{2n+1}{n(n+1)}. \tag{20}$$

The beam shape coefficients are expressed as simple integrals over the angular coordinate α

$$\begin{pmatrix} g^m_{n,\mathrm{TM}} \\ \mathrm{i}\, g^m_{n,\mathrm{TE}} \end{pmatrix} = (-1)^{m-1} \frac{1}{4} \frac{(n-|m|)!}{(n+|m|)!} \exp[\mathrm{i}k(z_1 - z_0)]$$
$$\times \int_0^{\pi/2} \exp(-\mathrm{i}k \cos\alpha\, z_1) \left[\Psi_{nm}(\alpha)\, T_{m-1}(\sin\alpha) \pm \Psi_{n,-m}(\alpha)\, T_{m+1}(\sin\alpha)\right]$$
$$\times \frac{1}{s^2} f(\sin\alpha) \exp\left(-\frac{1}{4\mathrm{i}\bar{Q}s^2}\sin^2\alpha\right) \sin\alpha \cos\alpha\, \mathrm{d}\alpha, \tag{21}$$

where

$$T_m(\alpha) = J_m(k\rho_0 \sin\alpha) \exp(\mathrm{i}m\varphi_0),$$
$$\Psi_{nm}(\alpha) = \frac{\mathrm{d}P_n^{|m|}(\cos\alpha)}{\mathrm{d}\alpha} \begin{pmatrix} \cos\alpha \\ 1 \end{pmatrix} + m \frac{P_n^{|m|}(\cos\alpha)}{\sin\alpha} \begin{pmatrix} 1 \\ \cos\alpha \end{pmatrix}, \tag{22}$$
$$f(\sin\alpha) = 1 + \sin^2\alpha - \frac{\sin^4\alpha}{16\mathrm{i}\bar{Q}s^2}.$$

We have denoted $\rho_0 = \sqrt{x_0^2 + y_0^2}$, $\varphi_0 = \arctan(x_0/y_0)$ and z_0 the cylindrical coordinates of the beam centre in the particle coordinate system. An inspection of Eq. (21) reveals that the numerical evaluation of the beam shape coefficients requires a procedure to compute Legendre functions and Bessel functions of integer order. The plane $z_1 = \mathrm{const}$ represents the plane where the boundary conditions were imposed. It seems to be reasonable to choose this plane to be the plane where the particle is located, also we assume $z_1 = 0$.

We have compared the values of some $g^m_{n,\mathrm{TM}}$ coefficients computed by the localized approximation method (mathematical expressions given in Refs. [17–19]) and by using the integral representation (21). For this calculation and for the following ones we have considered the case $w_0 = 5$ μm, $\lambda = 0.5$ μm, $x_0 = y_0 = 2$ μm and $z_0 = 10$ μm. A quantitative comparison of the localized approximation method and plane wave spectrum method concerning the values of the $g^m_{n,\mathrm{TM}}$ coefficients is given in Table 2. The relative errors are given in Fig. 2 for three azimuthal modes $m = 0$, 1, 2 and n ranging from 1 to 15. The cumulated relative differences for the real and imaginary part are less than 0.3%.

The exponential factor $\exp[-\sin^2\alpha/(4\mathrm{i}\bar{Q}s^2)]$ in the integrand ensures that the interval near $\alpha = 0$ provides the largest contribution to the integral. When the approximation of the Legendre functions [20]

$$P_n^{|m|}(\cos\alpha) \to \frac{(n+|m|)!}{(n-|m|)!} \frac{J_{|m|}[(n+0.5)\alpha]}{(n+0.5)^{|m|}} \tag{23}$$

is used for $\alpha \to 0$, the estimation

$$\Psi_{nm}(\alpha) \sin\alpha \approx \frac{(n-|m|)!}{(n+|m|)!}\, \hat{\Psi}_{nm}(\alpha), \tag{24}$$

where

$$\hat{\Psi}_{nm}(\alpha) = \frac{1}{(n+0.5)^{|m|}} \left\{ (n+1+|m|) \left(\frac{n+0.5}{n+1.5}\right)^{|m|} J_{|m|}[(n+1.5)\alpha] \right.$$
$$\left. - \left[(n+1)\,(1-\alpha^2/2) - m\right] J_{|m|}[(n+0.5)\,\alpha] \right\} \tag{25}$$

is valid in this limit.

We thus obtain a simplified integral representation for the beam shape coefficients

$$\begin{pmatrix} g^m_{n,\mathrm{TM}} \\ \mathrm{i}\, g^m_{n,\mathrm{TE}} \end{pmatrix} = (-1)^{m-1} \frac{\exp(-\mathrm{i}kz_0)}{4} \left\{ U_{nm} \exp[\mathrm{i}(m-1)\varphi_0] \pm V_{nm} \exp[\mathrm{i}(m+1)\varphi_0] \right\}, \tag{26}$$

where U_{nm} and V_{nm} are integral terms expressed as

$$U_{nm} = \int_0^1 \hat{\Psi}_{nm}(x)\, J_{m-1}(k\rho_0 x)\, \frac{1}{s^2} f(x) \exp\left(-\frac{x^2}{4\mathrm{i}\bar{Q}s^2}\right) \mathrm{d}x,$$
$$V_{nm} = \int_0^1 \hat{\Psi}_{n,-m}(x)\, J_{m+1}(k\rho_0 x)\, \frac{1}{s^2} f(x) \exp\left(-\frac{x^2}{4\mathrm{i}\bar{Q}s^2}\right) \mathrm{d}x. \tag{27}$$

Table 2
Comparison between the $g^m_{n,\mathrm{TM}}$ coefficients computed by the localized approximation method and the plane wave spectrum method. We have considered the case $w_0 = 5$ μm, $\lambda = 0.5$ μm, $x_0 = y_0 = 2$ μm, $z_0 = 10$ μm, three azimuthal modes $m = 0, 1, 2$ and n ranging from 1 to 5

m n	Localized approximation	PWSM – integral representation Eq. (21)	PWSM – integral representation Eq. (26)	PWSM – integral representation Eq. (26) – $f(x) = 1$
0	9.82726e-4	9.83249e-4	9.83251e-4	9.82586e-4
1	9.16325e-3	9.16566e-3	9.16567e-3	9.15986e-3
0	2.94447e-3	2.94604e-3	2.94639e-3	2.94320e-3
2	2.74665e-2	2.74738e-2	2.74760e-2	2.74586e-2
0	5.87785e-3	5.88097e-3	5.88192e-3	5.87555e-3
3	5.48635e-2	5.48780e-2	5.48839e-2	5.48491e-2
0	9.77181e-3	9.77697e-3	9.77878e-3	9.76818e-3
4	9.12850e-2	9.13089e-2	9.13201e-2	9.12622e-2
0	1.46116e-2	1.46193e-2	1.46223e-2	1.46064e-2
5	1.36638e-1	1.36674e-1	1.36692e-1	1.36605e-1
1	3.62323e-1	3.62508e-1	3.62505e-1	3.62332e-1
1	−1.57215e-2	−1.57653e-2	−1.57358e-2	−1.57185e-2
1	3.62064e-1	3.62248e-1	3.62246e-1	3.62073e-1
2	−1.57598e-2	−1.58036e-2	−1.57742e-2	−1.57568e-2
1	3.61676e-1	3.61860e-1	3.61857e-1	3.61685e-1
3	−1.58172e-2	−1.58609e-2	−1.58315e-2	−1.58141e-2
1	3.61159e-1	3.61342e-1	3.61340e-1	3.61168e-1
4	−1.58935e-2	−1.59370e-2	−1.59076e-2	−1.58903e-2
1	3.60514e-1	3.60696e-1	3.60694e-1	3.60522e-1
5	−1.59882e-2	−1.60316e-2	−1.60023e-2	−1.59850e-2
2	−2.53439e-3	−2.53751e-3	−2.53615e-3	−2.53443e-3
2	−2.04327e-3	−2.04515e-3	−2.04450e-3	−2.04331e-3
2	−2.53117e-3	−2.53428e-3	−2.53293e-3	−2.53121e-3
3	−2.04061e-3	−2.04249e-3	−2.04184e-3	−2.04066e-3
2	−2.52688e-3	−2.52998e-3	−2.52864e-3	−2.52692e-3
4	−2.03707e-3	−2.03895e-3	−2.03830e-3	−2.03712e-3
2	−2.52153e-3	−2.52460e-3	−2.52328e-3	−2.52157e-3
5	−2.03266e-3	−2.03453e-3	−2.03389e-3	−2.03271e-3

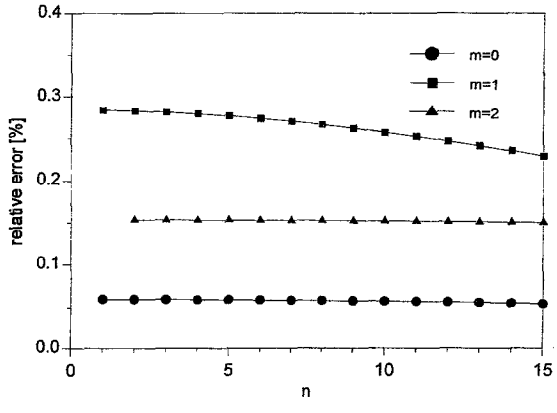

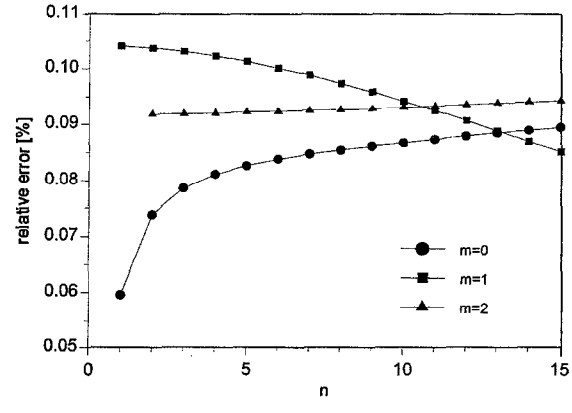

Fig. 2. Cumulated relative errors for the real and imaginary part of the $g^m_{n,\mathrm{TM}}$ coefficients computed by the localized approximation method and by using the integral representation given in Eq. (21). $w_0 = 5$ μm, $\lambda = 0.5$ μm, $x_0 = y_0 = 2$ μm, $z_0 = 10$ μm, $m = 0, 1, 2$, $n = 1, \ldots, 15$.

Fig. 3. Cumulated relative errors for the real and imaginary part of the $g^m_{n,\mathrm{TM}}$ coefficients computed by the localized approximation method and by using the simplified integral representation given in Eq. (26). $w_0 = 5$ μm, $\lambda = 0.5$ μm, $x_0 = y_0 = 2$ μm, $z_0 = 10$ μm, $m = 0, 1, 2$, $n = 1, \ldots, 15$.

We note that the integrands in Eq. (27) only contain Bessel functions of integer order and real arguments. The beam shape coefficients satisfy the following symmetry relations

$$\begin{aligned} &g^{-m}_{n,\mathrm{TM}}(x_0, y_0, z_0) = g^{m}_{n,\mathrm{TM}}(x_0, -y_0, z_0), \\ &g^{m}_{n,\mathrm{TE}}(x_0, y_0, z_0) = (-\mathrm{i})^m g^{m}_{n,\mathrm{TM}}(y_0, -x_0, z_0), \quad \text{for } m \geq 0, \\ &g^{-m}_{n,\mathrm{TE}}(x_0, y_0, z_0) = -g^{m}_{n,\mathrm{TE}}(x_0, -y_0, z_0), \quad \forall m. \end{aligned} \tag{28}$$

The integral terms U_{nm} and V_{nm} can be computed from each other by using the symmetry properties

$$V_{nm} = (-1)^{m+1} U_{n,-m}, \quad U_{nm} = (-1)^{m-1} V_{n,-m}, \quad m \geq 0. \tag{29}$$

The relative differences between the values of the $g^{m}_{n,\mathrm{TM}}$ coefficients computed in the localized approximation method and by using the simplified integral representation (26) are plotted in Fig. 3. The relative errors are less than 0.105%.

In our formulation, the beam shape coefficients are expressed as simple integrals. In contrast, since in the partial wave decomposition method the quadrature technique has to integrate over the particle surface, they are very time-consuming. But the main advantage of our representation consists in the fact that the beam shape coefficients only depend on the axial position of the plane, where the equivalence is considered. For arbitrarily shaped particles such a dependence is more convenient than a radial dependence.

4. Localized approximation to the beam shape coefficients

As mentioned before, the localized approximation of the beam shape coefficients represents an analytical approximation for a weakly focused Gaussian beam which simplifies and significantly speeds up numerical computations. The form of the analytical approximation was found in part by analogy to the propagation of geometrical light rays and in part by numerical experiments. A partial justification of the approximation from basic principles was given in the context of the partial wave decomposition method in Refs. [18,19]. By using the Taylor series expansions of the beam shape coefficients for a Davis first-order beam and for the localized approximation, the authors found an agreement up to and inclusively the s^{m+2} terms. The purpose of this section is to provide a complete demonstration of the localized approximation for on-axis and off-axis beams. The mathematical proof will be given for a weakly Gaussian beam starting from its plane wave spectrum representation.

For the Davis first-order beam approximation $f(x) = 1$ and the relative differences between the values of the $g^{m}_{n,\mathrm{TM}}$ coefficients computed by the localized approximation method and by using the simplified integral representation (26) are less than 0.055%. The curves in Fig. 4 show that the agreement between the two beam shape coefficient representations is perfect. It was surprising to find that the simplified integral representation is more closely related to the localized approximation than the integral representation (21). This numerical result leads to the conclusion that it will be possible to provide a justification of the localized approximation starting from Eq. (26) with $f(x) = 1$.

The most important advantage of the simplified integral representation consists in the fact that by using the series expansion of the Bessel functions and the basic integral [21]

$$\int_0^\infty \exp(-a^2 t^2)\, t^{\mu-1}\, J_\nu(bt) = \frac{\Gamma((\nu+\mu)/2)}{\Gamma(\nu+1)} \frac{1}{2a^\mu} \left(\frac{1}{2}\frac{b}{a}\right)^\nu M\big((\nu+\mu)/2,\, \nu+1,\, -b^2/4a^2\big) \tag{30}$$

the integration can be analytically performed to get a series representation for U_{nm} in terms of the confluent hypergeometric functions $M(\alpha, \beta, x)$

$$\begin{aligned} U_{nm} = {} & \frac{(\mathrm{i}\bar{Q})\,(\mathrm{i}\bar{Q}k\rho_0 s^2)^{m-1}}{|m|!} (\mathrm{i}\bar{Q}s^2)^{(|m|-m)/2} \\ & \times \big[(n+1+|m|)\, F_{m,0}(n+1.5) - (n+1-m)\, F_{m,0}(n+0.5) + 2(\mathrm{i}\bar{Q}s^2)\, F_{m,1}(n+0.5)\big], \end{aligned} \tag{31}$$

where

$$\begin{aligned} F_{m,p}(x) = {} & \sum_{k=0} \frac{(-\mathrm{i}\bar{Q}s^2k^2r_0^2)^k}{k!} \left[\frac{\Gamma((m+|m|)/2+k+p)}{\Gamma(m+k)}\right] \\ & \times M\big((m+|m|)/2+k+p,\, |m|+1, -\mathrm{i}\bar{Q}s^2x^2\big). \end{aligned} \tag{32}$$

For an on-axis Gaussian beam one can approximate

$$(n+2)\, M\big(1, 2, -s^2(n+1.5)^2\big) - n\, M\big(1, 2, -s^2(n+0.5)^2\big) \approx 2\exp\big[-s^2(n+0.5)^2\big] \tag{33}$$

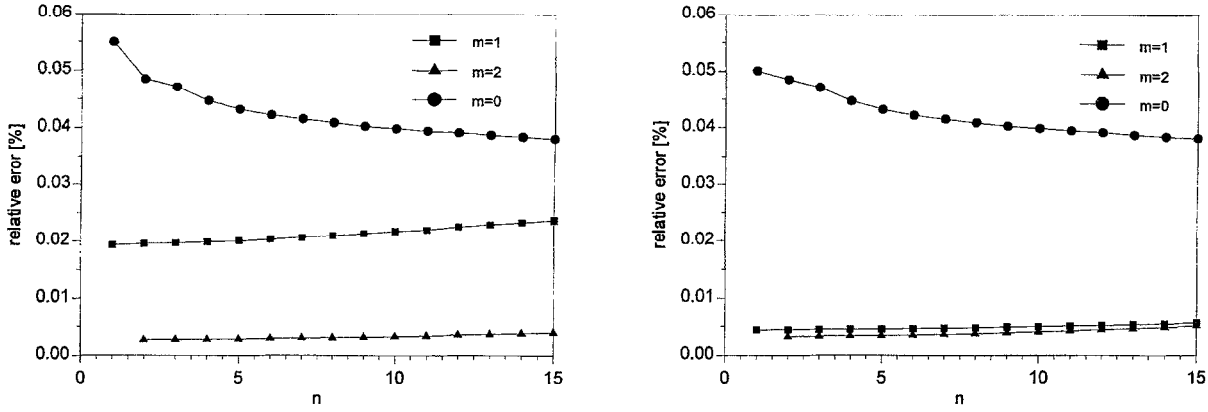

Fig. 4. Cumulated relative errors for the real and imaginary part of the $g_{n,\mathrm{TM}}^{m}$ coefficients computed by the localized approximation method and by using the simplified integral representation for the Davis first-order beam aproximation. $f(x)=1$, $w_0=5$ μm, $\lambda=0.5$ μm, $x_0=y_0=2$ μm, $z_0=10$ μm, $m=0,1,2$, $n=1,\ldots,15$.

Fig. 5. Cumulated relative errors for the real and imaginary part of the integral U_{nm} and the right-hand side of Eq. (35). $w_0=5$ μm, $\lambda=0.5$ μm, $x_0=y_0=2$ μm, $z_0=10$ μm, $m=0,1,2$, $n=1,\ldots,15$.

to obtain

$$\begin{aligned} &g_{n,\mathrm{TM}}^{1}\approx g_{n,\mathrm{TM}}^{1,\mathrm{loc}}=0.5g_n,\quad g_{n,\mathrm{TM}}^{-1}\approx g_{n,\mathrm{TM}}^{-1,\mathrm{loc}}=0.5g_n,\\ &g_{n,\mathrm{TE}}^{1}\approx g_{n,\mathrm{TE}}^{1,\mathrm{loc}}=-0.5\mathrm{i}\,g_n,\quad g_{n,\mathrm{TE}}^{-1}\approx g_{n,\mathrm{TE}}^{-1,\mathrm{loc}}=0.5\mathrm{i}\,g_n,\\ &g_n=\mathrm{i}\overline{Q}\,\exp\left[-\mathrm{i}\overline{Q}s^2(n+0.5)^2\right]\exp(-\mathrm{i}kz_0), \end{aligned} \tag{34}$$

which verifies the localized approximation on-axis for $z_0\neq 0$.

The form of Eq. (31) suggests that the integral U_{nm} may be estimated to be

$$U_{nm}\approx 2\,(-1)^{m-1}\,K_{nm}\,\overline{\Psi}_0^0\,J_{m-1}\left(2\overline{Q}\rho_0\rho_n/w_0^2\right), \tag{35}$$

where

$$\begin{aligned} &\overline{\Psi}_0^0=\mathrm{i}\overline{Q}\,\exp\left(-\mathrm{i}\overline{Q}\rho_0^2/w_0^2\right)\exp\left[-\mathrm{i}\overline{Q}(n+0.5)^2/\left(k^2w_0^2\right)\right],\\ &K_{nm}=\begin{cases}(-\mathrm{i})^{|m|}\mathrm{i}/(n+0.5)^{|m|-1}, & m\neq 0,\\ n(n+1)/(n+0.5), & m=0,\end{cases}\\ &\rho_n=(n+0.5)/k. \end{aligned} \tag{36}$$

A numerical evaluation of the integral U_{nm} and of the right-hand side of Eq. (35) shows that the relative differences are about 0.05% for $m=0$, and smaller as 0.01% for the other azimuthal modes. Therefore, in view of Fig. 5 we may conclude that the agreement is perfect.

According to the symmetry relations (29)

$$V_{nm}\approx 2\,(-1)^{m-1}\,K_{nm}\,\overline{\Psi}_0^0\,J_{m+1}\left(2\overline{Q}\rho_0\rho_n/w_0^2\right) \tag{37}$$

the beam shape coefficients can be simplified to

$$\begin{aligned} \begin{pmatrix} g_{n,\mathrm{TM}}^{m,\mathrm{loc}}\\ \mathrm{i}\,g_{n,\mathrm{TE}}^{m,\mathrm{loc}}\end{pmatrix}&\approx K_{nm}\overline{\Psi}_0^0\,\exp(-\mathrm{i}kz_0)\\ &\times\frac{1}{2}\left[\exp[\mathrm{i}(m-1)\varphi_0]J_{m-1}\left(2\frac{\overline{Q}\rho_0\rho_n}{w_0^2}\right)\pm\exp[\mathrm{i}(m+1)\varphi_0]J_{m+1}\left(2\frac{\overline{Q}\rho_0\rho_n}{w_0^2}\right)\right], \end{aligned} \tag{38}$$

which verifies the localized approximation for off-axis positions [22].

5. Numerical results

Our final test concerns the influence of the higher-order corrections of a Gaussian beam to the scattered field. We have computed the normalized differential scattering cross-section for a spheroidal particle with an axial ratio $a/b=2$, a size

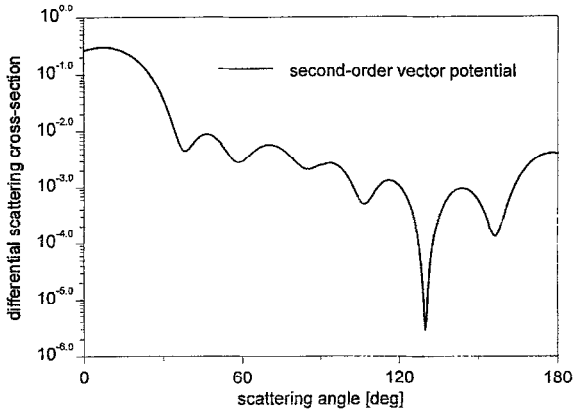

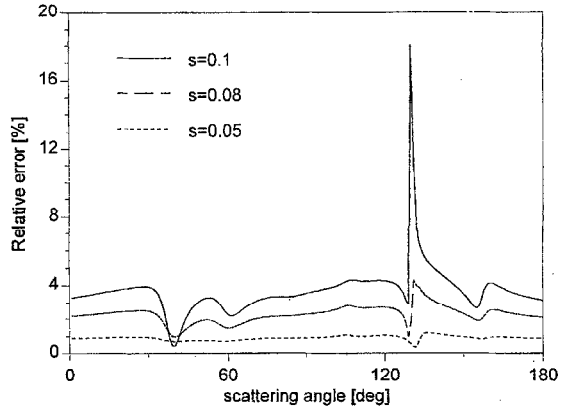

Fig. 6. Plots of the normalized differential scattering cross-section patterns for a spheroidal particle of $M = 1.5$, $a/b = 2$, $ka = 10$, having a position and an orientation given by $x_0 = y_0 = w_0/2$, $z_0 = w_0$ and $\alpha = \beta = 0$. The Gaussian beam parameter is $s = 0.1$. The curve corresponds to the second-order approximation of the vector potential.

Fig. 7. Relative error of the differential scattering cross-section corresponding to the zeroth- and the second-order approximation of the vector potential. Three values of the beam parameter s are considered: 0.05, 0.08 and 0.1.

parameter $ka = 10$, and an index of refraction of 1.5 by using the extended boundary condition method. The incident wave is linearly polarized in the x-direction. In this case the angular scattering will be evaluated for parallel polarization over the azimuthal plane, i.e. the $\varphi = 0$ plane. The scattering object is located at the coordinates $x_0 = y_0 = w_0/2$ and $z_0 = w_0$ with respect to the beam coordinate system. The symmetry axis of the particle is along the incident direction, i.e. the Euler orientation angles are taken to be $\alpha = 0$ and $\beta = 0$. We note that for an arbitrary orientation of the particle we use an addition theorem for spherical vector wave functions under coordinate rotations to compute the beam shape coefficients in the particle system [22]. The beam shape coefficients are computed by using the integral representation (26) for the zeroth- and the second-order approximations of the vector potential. For the zeroth-order vector potential we take $f(x) = 1$ and, since this was mentioned before this representation is very closely related to the localized approximation and the classical plane wave spectrum representation. The normalized differential scattering cross-section pattern is shown in Fig. 6 for a Gaussian beam with $s = 0.1$. The curve corresponds to the second-order approximation of the vector potential. In Fig. 7 we have plotted the relative error of the differential scattering cross-section for the zeroth- and the second-order approximation of the vector potential. The data points correspond to three values of the beam parameter s: 0.05, 0.08 and 0.1. The results show that the relative error is about 1% for $s = 0.05$ but about 4% for $s = 0.1$. The peak of about 20% in the error curve has no significant importance since this deviation is at a level of 10^{-5} of the maximum scattered field. From the previous analysis, it might be concluded that for tightly focused Gaussian beams the second-order approximation of the vector potential yields a significant improvement in accuracy.

6. Conclusions

A plane wave spectrum method of Gaussian beams can be constructed by using Davis' approximations for the vector potential and the inverse Fourier transform of the spectrum function of the original vector potential in a given plane to define an equivalent vector potential which satisfies the wave equation. By using the higher-order terms in the expansion of the vector potential we are able to evaluate the higher-order corrections of the equivalent electromagnetic field. The electric field, which corresponds to the equivalent vector potential, satisfies the vector wave equation, is divergence free and can be written as a sum of plane waves.

The electromagnetic character of the equivalent incident field offers the possibility to perform an expansion in terms of spherical vector wave functions of the first kind. For the beam shape coefficients we have derived several integral representations. The values obtained from the integral representation computations agree with the values obtained by the localized approximation for off-axis Gaussian beams. For a Davis first-order beam we have proved the localized approximation for on-axis and off-axis Gaussian beams. The most important result is the identity, except an insignificant factor, between the integral representation for the beam shape coefficients obtained in our version of the plane wave spectrum method and by using a translational addition theorem for spherical vector wave functions [23].

Acknowledgements

The autors are grateful to the DFG (Deutsche Forschungsgemeinschaft) for providing financial support for this work. The comments provided by the reviewers were greatly appreciated.

References

[1] P.W. Barber and S.C. Hill, Light scattering by particles: computational methods (World Scientific, Singapore, 1990).
[2] G. Gouesbet and G. Grehan, J. Opt. (Paris) 13 (1982) 97.
[3] G. Gouesbet, G. Grehan and B. Maheau, J. Opt. (Paris) 16 (1985) 89.
[4] G. Grehan, B. Maheau and G. Gouesbet, Appl. Optics 25 (1986) 3539.
[5] G. Gouesbet, B. Maheau and G. Grehan, J. Opt. Soc. Am. A 5 (1989) 1427.
[6] J.P. Barton, D.R. Alexander and S.A. Schaub, J. Appl. Phys. 64 (1988) 1632.
[7] E.E.M. Khaled, S.C. Hill and P.W. Barber, IEEE Trans. Antennas Propag. (1993) 41.
[8] E.E.M. Khaled, Ph.D. Thesis, Clarkson University, 1993.
[9] S. Colak, C. Yeh and L.W. Casperson, Appl. Optics 18 (1979) 294.
[10] C. Yeh, S. Colak and P. Barber, Appl. Optics 21 (1982) 4426.
[11] P. Barber and C. Yeh, Appl. Optics 14 (1975) 2864.
[12] L.W. Davis, Phys. Rev. A 19 (1979) 1177.
[13] H. Kogelnik and T. Li, Appl. Optics 5 (1969) 1550.
[14] J.W. Goodman, Introduction to Fourier Optics (McGraw-Hill, New York, 1968).
[15] J.P. Barton and D.R. Alexander, J. Appl. Phys. 7 (1989) 2800.
[16] J.A. Stratton, Electromagnetic theory (Mc Graw-Hill, New York, 1941).
[17] G. Gouesbet, G. Grehan and B. Maheau, J. Opt. Soc. Am. A 7 (1990) 998.
[18] J.A. Lock and G. Gouesbet, J. Opt. Soc. Am. A 11 (1994) 2503.
[19] G. Gouesbet and J.A. Lock, J. Opt. Soc. Am. A 11 (1994) 2516.
[20] J.A. Lock, J. Opt. Soc. Am. A 10 (1993) 693.
[21] M. Abramowitz and I.A. Stegun, Handbook of mathematical functions (Dover, New York, 1972).
[22] A. Doicu, S. Schabel and F. Ebert, Part. Part. Syst. Charact. 13 (1996) 79.
[23] A. Doicu and T. Wriedt, Computation of the beam shape coefficients in generalized Lorenz-Mie theory using the translational addition theorem for spherical vector wave functions, Appl. Optics, submitted.